remote sensing

MDPI

Article

Estimating Changes in Leaf Area, Leaf Area Density, and Vertical Leaf Area Profile for Mango, Avocado, and Macadamia Tree Crowns Using Terrestrial Laser Scanning

Dan Wu [1,2,*], Stuart Phinn [1,2], Kasper Johansen [2,3], Andrew Robson [2,4], Jasmine Muir [1,2,4,5] and Christopher Searle [6]

1 Remote Sensing Research Centre, School of Earth and Environmental Sciences, the University of Queensland, Brisbane, QLD 4072, Australia; s.phinn@uq.edu.au (S.P.); Jasmine.Muir@astron.com.au (J.M.)
2 The Joint Remote Sensing Research Program, Brisbane, QLD 4072, Australia; Kasper.Johansen@kaust.edu.sa (K.J.); andrew.robson@une.edu.au (A.R.)
3 Water Desalination and Reuse Center, King Abdullah University of Science and Technology, Thuwal 23955-6900, Saudi Arabia
4 Precision Agriculture Research Group (PARG), University of New England, Armidale, NSW 2351, Australia
5 Astron Environmental Consulting, 129 Royal Street, East Perth, WA 6004, Australia
6 MacAvo Consulting, 84 Pashleys Road, Bundaberg, QLD 4670, Australia; MacAvoConsulting@bigpond.com
* Correspondence: d.wu@uqconnect.edu.au; Tel.: +61-7-3365-6524

Received: 2 October 2018; Accepted: 2 November 2018; Published: 6 November 2018

Abstract: Vegetation metrics, such as leaf area (LA), leaf area density (LAD), and vertical leaf area profile, are essential measures of tree-scale biophysical processes associated with photosynthetic capacity, and canopy geometry. However, there are limited published investigations of their use for horticultural tree crops. This study evaluated the ability of light detection and ranging (LiDAR) for measuring LA, LAD, and vertical leaf area profile across two mango, macadamia and avocado trees using discrete return data from a RIEGL VZ-400 Terrestrial Laser Scanning (TLS) system. These data were collected multiple times for individual trees to align with key growth stages, essential management practices, and following a severe storm. The first return of each laser pulse was extracted for each individual tree and classified as foliage or wood based on TLS point cloud geometry. LAD at a side length of 25 cm voxels, LA at the canopy level and vertical leaf area profile were calculated to analyse tree crown changes. These changes included: (1) pre-pruning vs. post-pruning for mango trees; (2) pre-pruning vs. post-pruning for macadamia trees; (3) pre-storm vs. post-storm for macadamia trees; and (4) tree leaf growth over a year for two young avocado trees. Decreases of 34.13 m^2 and 8.34 m^2 in LA of mango tree crowns occurred due to pruning. Pruning for the high vigour mango tree was mostly identified between 1.25 m and 3 m. Decreases of 38.03 m^2 and 16.91 m^2 in LA of a healthy and unhealthy macadamia tree occurred due to pruning. After flowering and spring flush of the same macadamia trees, storm effects caused a 9.65 m^2 decrease in LA for the unhealthy tree, while an increase of 34.19 m^2 occurred for the healthy tree. The tree height increased from 11.13 m to 11.66 m, and leaf loss was mainly observed between 1.5 m and 4.5 m for the unhealthy macadamia tree. Annual increases in LA of 82.59 m^2 and 59.97 m^2 were observed for two three-year-old avocado trees. Our results show that TLS is a useful tool to quantify changes in the LA, LAD, and vertical leaf area profiles of horticultural trees over time, which can be used as a general indicator of tree health, as well as assist growers with improved pruning, irrigation, and fertilisation application decisions.

Keywords: terrestrial laser scanning; horticultural; leaf area; leaf area density; vertical leaf area profile

1. Introduction

Light detection and ranging (LiDAR) is an active remote sensing technology. A laser scanner emits laser pulses to precisely and accurately measure distances between the scanner and each survey point based on the speed of light and the time each laser pulse travels. Airborne laser scanning (ALS) data can provide canopy structure measurements over a large area, whist terrestrial laser scanning (TLS) data can be used to obtain detailed canopy scale measurements [1]. Most TLS applications are currently focused on structural engineering and forest structure mapping [1–5]. Previous studies have demonstrated that TLS can accurately calculate forest structure at voxel level, individual tree level, and plot level [1,6,7]. Srinivasan et al. [8] presented an automatic method to accurately calculate tree height, crown width and diameter at breast height (DBH) at an individual tree level from TLS data. Jupp et al. [9] developed a method to consistently calculate leaf area index (LAI) and forest plant area volume density (PAVD) from TLS data, which showed potential of TLS as a ground data source to calibrate these measurements from other remote sensing platforms, such as airborne and spaceborne platforms. Calders et al. [10] later proved that correcting topography was essential for LAI and PAVD calculations from TLS, whilst Kaasalainen et al. [11] and Calders et al. [12] combined TLS measurements and three-dimensional (3D) quantitative structure modelling [13] to produce robust and highly accurate aboveground biomass calculations. TLS data has also been applied to calibrate and validate vegetation structure and biomass calculations from ALS data [14,15].

Canopy structure metrics are closely related to horticultural tree growth and productivity, as well as providing strong indicators of water consumption, health condition and yield [16–19]. Leaf area (LA) calculations are essential to determine water requirements for precision irrigation and fertilisation [16]. Accurate LA calculations can optimise the dosage of pesticide, fertiliser, and water, and also measure plant scale responses to these applications [16,20]. As such, canopy structure metrics, including volume, foliage and LAI, have important applications in crop training, irrigation, fertilisation, and pesticide application for horticultural tree crops [16]. Crop training such as pruning and thinning techniques are used to improve light penetration and air circulation, which affect fruit colour and sugar levels [21]. Hence canopy structure information at the individual tree level can provide valuable information to support precision orchard management [16].

Previous studies on LA, leaf area density (LAD) and vertical leaf area profile calculations using high spatial resolution TLS have generally focused on forestry [2,3,9,22], with some examples of TLS with sparse point clouds being evaluated on horticultural tree crops [16,23–26]. Based on previous research, high spatial resolution TLS is essential to accurately classify leaves and branches [27,28]. However, to assist in the development of improved management practices, such as targeted limb removal and the variable rate application of foliar sprays, it is essential that high spatial resolution TLS also be evaluated for the accurate measure of LA and LAD within horticultural tree crops [29]. Even with the potential to apply variable rate pesticide based on LA at different tree height and other supplementary data, most fertiliser and pesticide applications use the same dose for whole tree rows [20].

In Australia, the canopy row method for variable rate spray applications was developed for fruit trees and vines to adjust water volume according to canopy height and width, as well as row length [30]. By using this method together with improved coverage sprayers and on-target spray technology, chemical usage was reduced by approximately 50% [30]. An easy and accurate calculation of LA is a key parameter for spray application adjustment [29]. However, there is no research in Australia on spray application for horticultural tree crops based on LA and LAD. In contrast, canopy structure metrics including LA and LAD have been recognised as important parameters for spray dosage adjustment in horticultural research in Europe [31,32]. LAD is a 3D measurement that integrates total LA in a canopy, and it also illustrates the spatial distribution of LA either within a canopy or a given volume [6,33]. LAD relates directly to light interception and the variance of LAD indicates the leaf distribution. Optimising leaf distribution can maximise photosynthetic performance for horticultural tree crops [16,18].

Our study aimed to calculate tree level LA, voxel (25 cm in side length) LAD, and vertical leaf area profiles using TLS for mango, avocado, and macadamia tree crops. This information provides the foundation to develop orchard management plans tailored to individual trees, such as precision spray dosages and pruning based on the LA at a particular height for each tree. Data from this study was analysed based on canopy changes due to management and growth requirements.

2. Study Area and Data Collection

2.1. Study Area

For this study, two mango (*Mangifera indica*) cv. Calypso, two macadamia (*Macadamia integrifolia*) cv. HAES 344, and two avocado (*Persea americana*) cv. Hass trees, were selected from commercial orchards and a research station, near the township of Bundaberg, Australia (Figure 1). The Bundaberg region was selected for this study, as it is one of the largest horticulture regions in Australia, producing a large variety of fruit and nuts from tree crops [34]. For mango production, Queensland and the Northern Territory account for about 95% of Australia's total mango crops [35]. Along with the Burdekin and Mareeba regions, Bundaberg is one of the three main mango producing regions in Queensland [36], and one of the three major avocado production regions in Australia [37,38]. The Bundaberg region became the largest macadamia producing region in Australia in 2016, accounting for >30% of Australia's macadamia production [39].

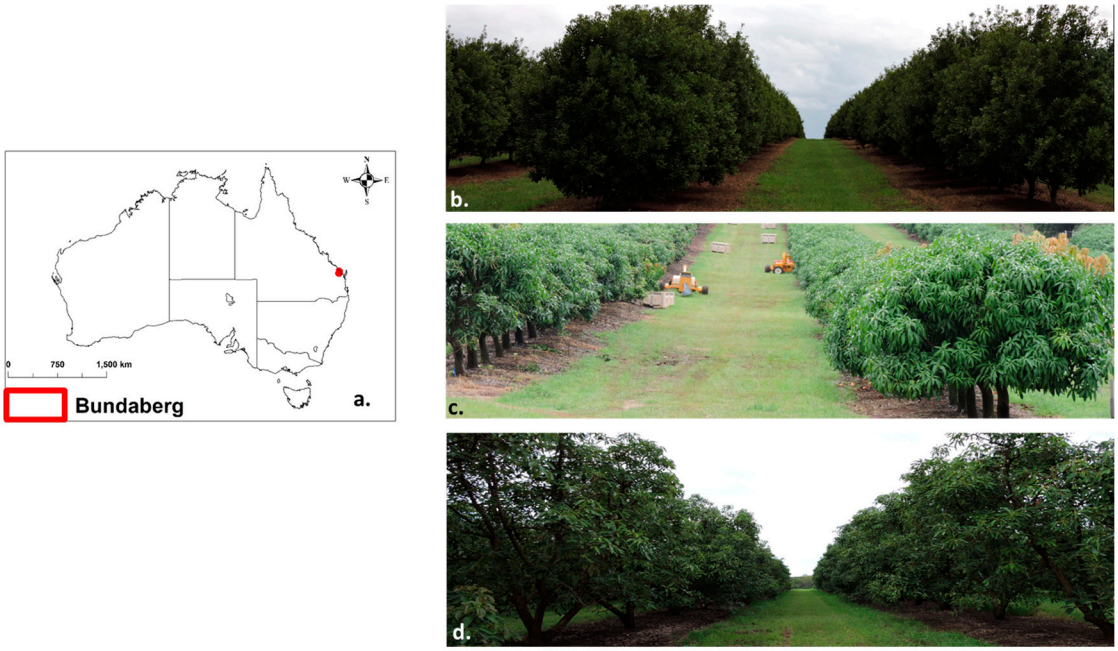

Figure 1. Location of the study area (**a**), pictures of a macadamia orchard (**b**), a mango orchard (**c**), and an avocado orchard (**d**) as examples.

2.2. LiDAR Data and Fieldwork Design

To calculate LAD, TLS data were collected with a RIEGL VZ-400 laser scanner (RIEGL, Horn, Austria), which was mounted on a tripod at a height of approximately 1.5 m. With a laser wavelength of 1550 nm in the near infrared part of the spectrum and a beam divergence of 0.35 mrad, the RIEGL VZ-400 scanner sends laser pulses up to a distance of 350 m, and records up to four returns per emitted pulse. Through inclination sensors and an internal compass, the RIEGL VZ-400 also collects pitch, roll, and yaw information. For this study, the RIEGL VZ-400 settings were the same for all scan locations and seasons. The laser scanner setting information is provided in Table 1. The appropriate laser point

sampling space should be selected based on the leaf size and shape of each tree type in the future, because leaf size is a critical factor which determines the sampling space [40].

Table 1. RIEGL VZ-400 scanner settings for data acquisition.

Beam divergence	0.35 mrad (i.e., at the range of 50 m the beam footprint size = 0.0175 m)
Pulse repetition rate	300 kHz
Minimum range	1.5 m
Maximum range	160 m (at 20% target reflectance) 350 m (at 90% target reflectance)
Azimuth range	0–360° (0.06° angular sampling)
Zenith range	30–130° (0.06° angular sampling)
Recorded data	Full waveform & up to four returns per emitted pulse

TLS data were collected under different conditions (Table 2) to assess changes in LA. One high and one low vigour (based on health and size [41]) mango tree were scanned pre-pruning and post-pruning on 3 February 2017. One healthy macadamia tree and one with Abnormal Vertical Growth (AVG) were scanned pre-pruning and post-pruning on 5 and 6 May 2016 and 14 August 2016, respectively. The same two macadamia trees were also scanned before (6 September 2017) and after (16 December 2017) a severe storm event. This isolated severe storm event, with strong wind gusts up to 98 km/h and heavy rain occurred across the study area on 7 November 2017. A wind direction of west to southwest was recorded. This uprooted trees, ripped off building roofs and brought down power lines [42]; TLS data were also collected 13 months apart for two young avocado trees on 15 August 2016 and 7 September 2017.

To minimize the occlusion issue from blocked TLS pulses, each tree was scanned from four locations during each sampling event (Figure 2). Additionally, due to the narrow row space, tree heights and the zenith angle (30–130°) of the RIEGL VZ-400 instrument, a vertical and a 90° tilt scan were conducted at each scan location for macadamia trees to ensure that the entire tree was scanned. Therefore, this included a total of four TLS scans per tree for mango and avocado trees and eight TLS scans per tree for macadamia trees for each sampling event. Multiple cylindrical reflectors were set up around each tree to ensure each two scans included at least the same four reflectors for coregistration between scan locations. All scans were collected during no or low wind conditions to ensure movement of leaves and branches between the eight scans was minimal. Hourly wind speeds were acquired from Bundaberg Aero weather station (24.9069°S, 152.3230°E) approximately 11 km from the macadamia orchard and two young avocado trees and 36 km from the mango orchard. The average hourly wind speed for the scans was between 13.86 km/h and 18.31 km/h, with the exception of the 14 and 15 August 2016, when the hourly wind speeds were 20.09 km/h and 29.68 km/h separately. However, as most trees within the orchards were sheltered from wind effects by surrounding trees, little to no movement of leaves and branches were observed during scanning. As a result of temporal changes in canopy structure from phenological growth stages and from mechanical operations (pruning), scan locations varied slightly between sampling dates. To register multi-temporal TLS datasets, four permanent ground control points were set up around each tree. A survey bipod fitted with a reflector was placed over each permanent survey marker at a height offset of 1.75 m to the ground control point with the assistance of the levelling bubble.

Table 2. Leaf area changes of mango, avocado, and macadamia trees, because of pruning, growth, and a storm.

Tree Type	1st Time Leaf Area (m^2)	1st Time Tree Height (m)	2nd Time Leaf Area (m^2)	2nd Time Tree Height (m)	Cause of Change	3rd Time Leaf Area (m^2)	3rd Time Tree Height (m)	4th Time Leaf Area (m^2)	4th Time Tree Height (m)	Cause of Change
Mango (high vigour)	76.41 Date: 3 February 2017	3.87	42.28 Date: 3 February 2017	3.46	Pruning	NA	NA	NA	NA	NA
Mango (low vigour)	27.94 Date: 3 February 2017	2.89	19.60 Date: 3 February 2017	2.89	Pruning	NA	NA	NA	NA	NA
Macadamia (healthy)	105.50 Date: 5 May 2016	7.94	67.47 Date: 14 August 2016	6.48	Pruning	60.33 Date: 6 September 2017	8.06	94.52 Date: 16 December 2017	9.05	Flowering and spring flush
Macadamia (AVG)	92.80 Date: 6 May 2016	11.34	75.89 Date: 14 August 2016	11.13	Pruning	91.21 Date: 6 September 2017	11.13	81.56 Date: 16 December 2017	11.66	Flowering, spring flush and storm damage
Avocado Tree1	40.03 Date: 15 August 2016	3.66	122.62 Date: 7 September 2017	5.17	Growth	NA	NA	NA	NA	NA
Avocado Tree 2	41.97 Date: 15 August 2016	3.60	101.94 Date: 7 September 2017	4.96	Growth	NA	NA	NA	NA	NA

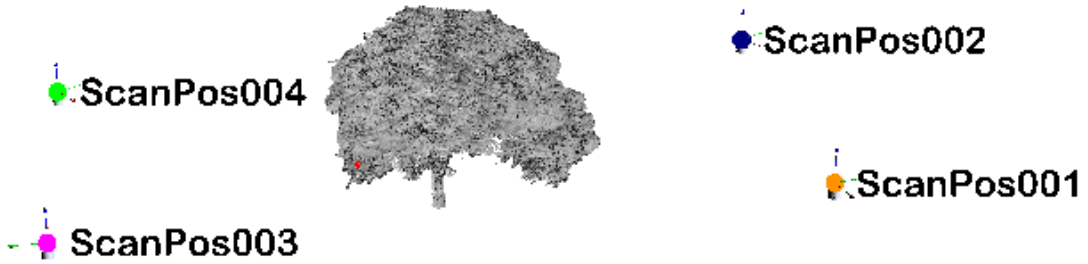

Figure 2. A 3D intensity image of a mango tree and four scan locations around it.

3. Methods

3.1. Data Registration

TLS scans collected for the same tree across multiple times (Table 2) over each growing season were co-registered to the same coordinate system to enable comparison over time. A reference TLS scan for each tree was first selected. Then the RiSCAN PRO (RIEGL, Horn, Austria) coarse registration tool was used to register one of the TLS scans from another date to the reference scan using the four permanent bipods' locations. The reflector-targets measured in the TLS scans from each separate position were then used to register other scan positions. To further improve registration, the Multi Station Adjustment tool in RiSCAN PRO was also applied.

3.2. Data Classification and Extraction

The first return of each laser pulse was extracted and then classified into leaves and branches based on their 3D geometrical properties. The CANUPO segmentation algorithm provided by the CloudCompare™ software (version 2.9.1, General Public License software, http://www.cloudcompare.org/) was used to establish training point clouds for both leaves (represented as identifier (1) and branches (represented as identifier (2)) [28]. The CANUPO segmentation algorithm classified each point using multi-scale measures of the point cloud dimensionalities around each point, the point cloud geometry at a given location and given scales. Class separability, spatial resolution, and the probabilistic confidence of the classification for each point at each scan location were then calculated [28]. The detailed classification parameters are described in Table 3. To speed up the computing time, we selected 5000–8000 points as a sub-sample (core points) (Table 3) for the local neighbourhoods computation. For each laser point, a neighbourhood sphere was computed at each scale of interest where the diameter of the sphere represented the scale. The scale in this study ranged from 0.01 m to 1 m at 0.1 m intervals. The best combination of scales with different weights was chosen automatically. Then the algorithm selects the best combination of scales and a local dimensionality (line, plane, or whole volume) which gives the greatest separability between classes. Both a balanced accuracy (ba) and Fisher discriminant ratio (fdr) were used to assess the classification results. A high ba value indicates a good recognition rate of a classifier on a given dataset (Table 3). A large fdr value implies a good separation between classes (Table 3).The extraction of TLS point clouds for mango trees and young avocado trees was more achievable than the similar process conducted on large macadamia trees due to their overlapping, continuous hedgerow canopy. Therefore, a bounding box was created for each macadamia tree, which was then repeatedly used to extract multi-date TLS data for the same tree.

Table 3. CANUPO segmentation parameters in the CloudCompare™ software for mango, macadamia, and avocado tree crops.

Tree Type	Classes	Scales (m)	Max Core Points	Balanced Accuracy	Fisher Discriminant Ratio (fdr)
Mango	Class 1: Leaves Class 2: branches	Min = 0.01, Max = 1, Step = 0.1	5000	99%	12.99
Macadamia	Class 1: Leaves Class 2: branches	Min = 0.01, Max = 1, Step = 0.1	5000	94%	5.54
Avocado	Class 1: Leaves Class 2: branches	Min = 0.01, Max = 1, Step = 0.1	8000	99%	10.99

3.3. Leaf Area, Leaf Area Density, Vertical Leaf Area Profile Calculation, and Voxel Size Effects Analysis

LA at the canopy level and LAD at a side length of 25 cm voxels were calculated for each of the mango, macadamia and avocado trees. LA refers to the one-sided area of the total leaf surface

area. Assuming that leaves are randomly distributed, LAD represents the one-sided LA measured in m^2 per volume measured in m^3. The vertical leaf area profile is the sum of LA calculated in m^2 for each 25 cm horizontal layer. LAD estimates were calculated from the VoxLAD model based on the statistics of transmission and interception of TLS laser pulses through each voxel (a 3D equivalent of pixel) [6]. The mean absolute percent error was found to be 6% by Béland et al. [6] compared to the complex ray-tracing simulations method presented by Béland et al. [22], which has an average 14% from the reference direct field LA measurements from leaves harvesting. To investigate the effect of voxel size on the LA calculation, we used 17 voxel sizes (10–90 cm, with a 5 cm interval) to calculate the LA changes on a young avocado tree. Many factors can influence the optimal voxel resolution, such as scan divergence, scan resolution and leaf size [43]. The validation of using the VoxLAD model to calculate mango, avocado, and macadamia LA should be further studied in the future. A voxel side length of 25 cm was chosen for the LAD calculation for all the tree crops in this study.

4. Results

The LA changes calculated from TLS data were caused by canopy management, growth or a severe storm. After pruning, LA dropped from 76.41 m^2 to 42.28 m^2 for the high vigour mango tree and from 27.94 m^2 to 19.60 m^2 for the low vigour mango tree (Table 2). Pruning for the high vigour mango tree was mostly identified between 1 m and 2.75 m (Figure 3e). Vertical leaf area loss between 0.62 m^2 and 7.98 m^2 were detected within this height, where the maximum LA decrease occurred at a height of approximately 2.25 m (Figure 3e). In contrast, the vertical leaf area loss ranged from 0.68 m^2 to 1.65 m^2 within the height of 1.5 m and 2.5 m for the low vigour mango tree. The standard deviation of the voxel level LAD of the high vigour and low vigour mango trees decreased from 5.17 m^2/m^3 to 3.37 m^2/m^3 (Figure 3d,d′) and 4.35 m^2/m^3 to 3.42 m^2/m^3 separately. Mango growers selectively remove dense branches and foliage in the centre of the canopy to promote air ventilation, spray and light penetration. LAD observations at 2 m and 3 m above ground height of the high vigour mango tree in Figure 4 exhibits the outcome of this management practice, with the centre of the canopy opened up after pruning.

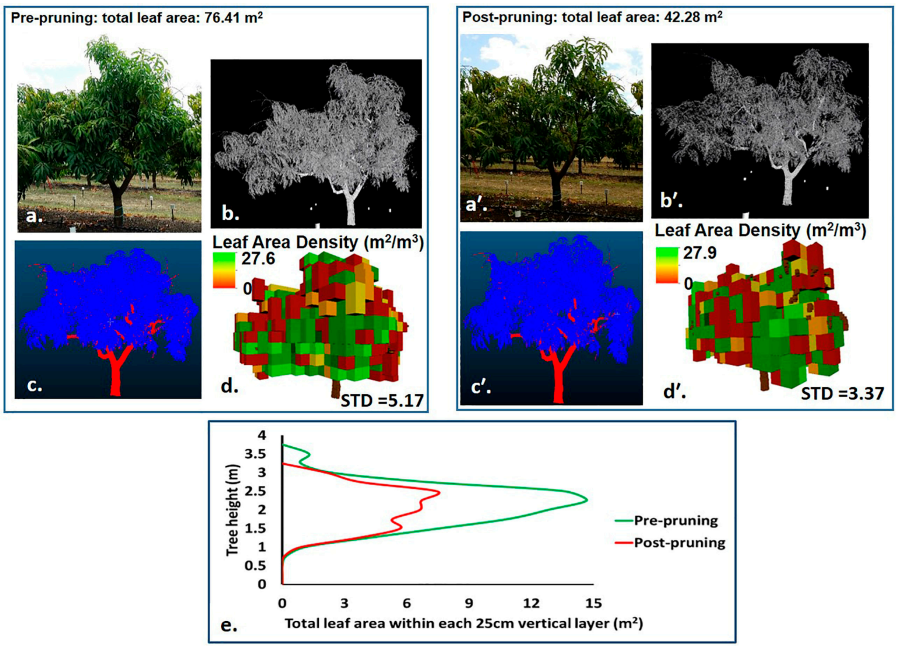

Figure 3. Pictures of the high vigour mango tree at two different points in time, i.e., pre-pruning = 3 February 2017, post-pruning = 3 February 2017 (**a**,**a′**), its corresponding 3D intensity images (**b**,**b′**) and classified discrete point clouds (**c**,**c′**), LAD at a voxel level (25 cm in side length) (**d**,**d′**), and vertical leaf area profile within each 25 cm vertical layer of pre-pruning and post-pruning.

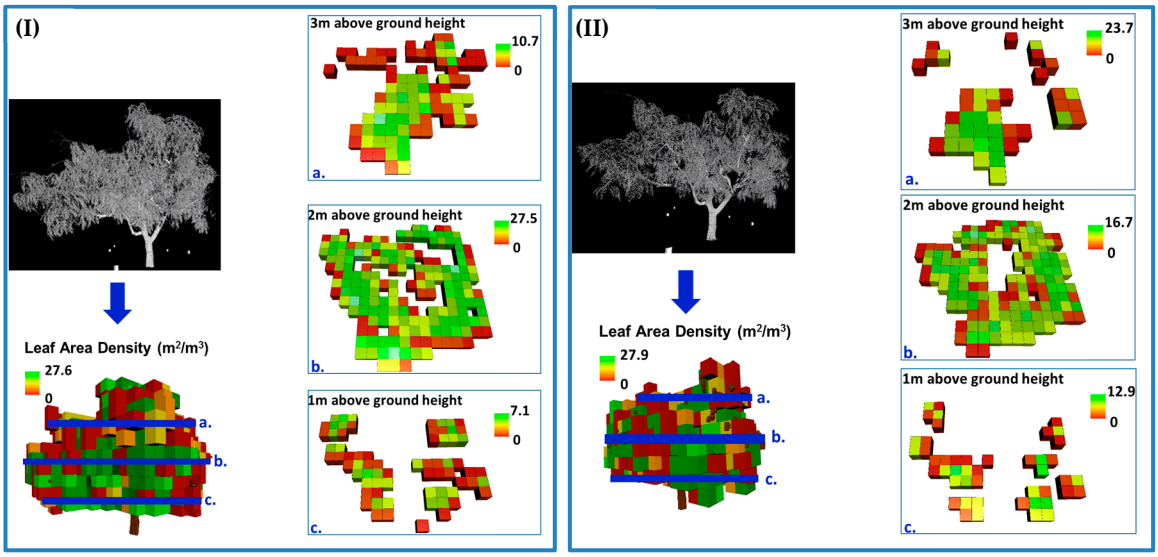

Figure 4. Intensity images of the high vigour mango tree at two different points in time, pre-pruning = 3 February 2017 (**I**), post-pruning = 3 February 2017 (**II**), leaf area density (LAD) of the entire tree crown, and LAD at 1 m, 2 m and 3 m above ground height at a voxel level (25 cm in side length).

The healthy macadamia tree decreased its LA from 105.50 m^2 to 67.47 m^2 after pruning and the macadamia tree with AVG in the same orchard decreased from 92.80 m^2 to 75.89 m^2 (Table 2). The standard deviation of voxel level LAD deceased from 2.27 m^2/m^3 to 0.95 m^2/m^3 for the healthy macadamia tree and, similarly, from 2.23 m^2/m^3 to 0.80 m^2/m^3 for the macadamia tree with AVG. Pre-storm and post-storm scans were collected on the 6 September and 16 December, 2017 respectively, within which the macadamia trees in this orchard experienced peak flowering and spring leaf flush. LA declined from 91.21 m^2 to 81.56 m^2 for the macadamia tree with AVG following a severe storm, while an LA increase from 60.33 m^2 to 94.52 m^2 was observed for the healthy macadamia tree (Table 2), which did not exhibit visible damage from the storm. After the storm, the standard deviation of voxel level LAD decreased from 1.39 m^2/m^3 to 1.11 m^2/m^3 for the macadamia tree with AVG (Figure 5d,d′). Leaf loss was mainly observed between 1.25 m and 4.5 m above ground height for the macadamia tree with AVG (Figure 5e). Within this height interval (1.25–4.5 m), vertical leaf area loss ranged from 0.56 m^2 to 2.39 m^2 for the macadamia tree with AVG (Figure 5e). Unfortunately, due to the occlusion effect, the results may also indicate an inability of the TLS to collect data from the centre of the canopy of macadamia trees at 3 m and 6 m above ground height (Figure 6). This can be either caused by the branches at the centre of the canopy having no leaves, or the occlusion effect, i.e., the laser beams were intercepted by the dense canopy, so they could not reach the centre of the canopy. Therefore, even with four scan locations established around each tree, the results suggest that occlusion may still be an issue in the collection of ground-based TLS data.

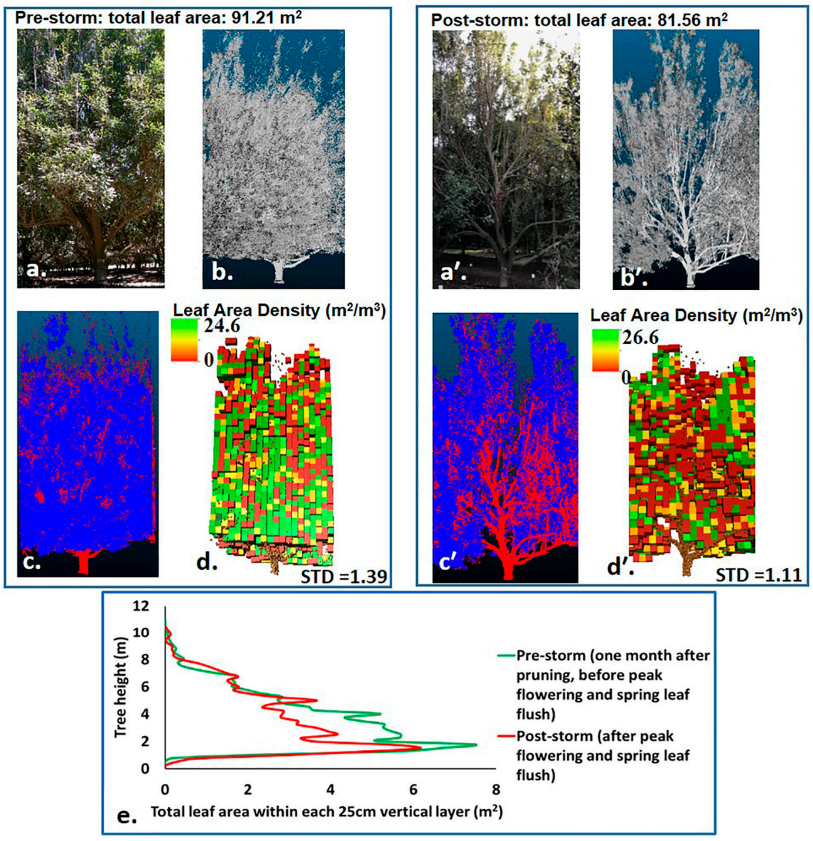

Figure 5. Pictures of a single macadamia tree with AVG at two different points in time, i.e., pre-storm = 6 September 2017, post-storm = 16 December 2017 (**a**,**a′**), its corresponding TLS 3D intensity images (**b**,**b′**), classified point cloud (**c**,**c′**), leaf area density (LAD) at a voxel level (25 cm in side length) (**d**,**d′**), and vertical leaf area profile within each 25 cm vertical layer of pre-storm and post-storm (**e**).

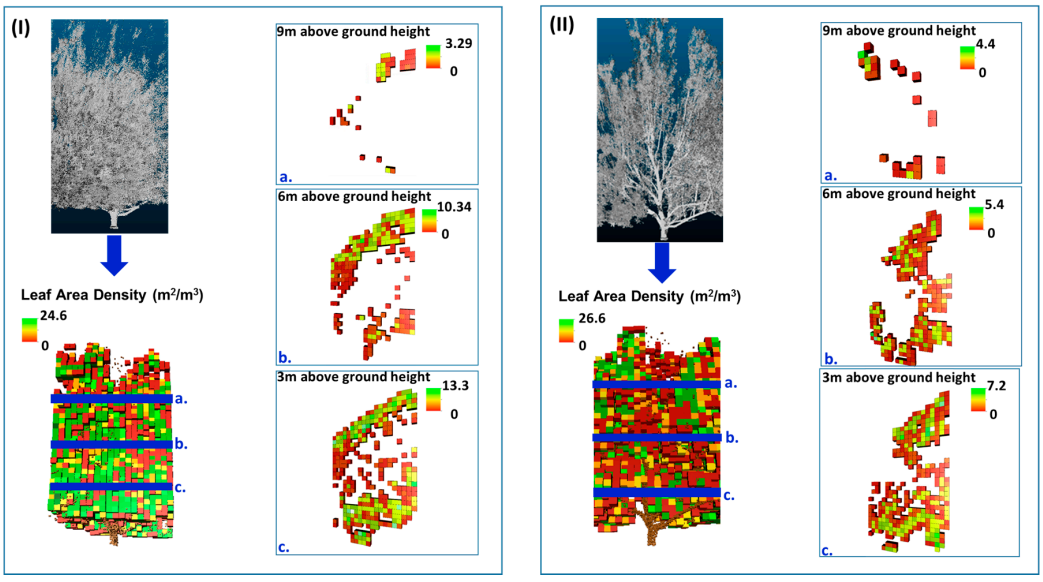

Figure 6. 3D intensity images of a single macadamia tree with AVG at two different points in time, i.e., pre-storm = 6 September 2017 (**I**), post-storm = 16 December 2017 (**II**), its corresponding leaf area density (LAD) of the entire tree crown, and LAD at 3 m, 6 m, and 9 m above ground height at a voxel level (25 cm in side length).

We found that LA of the two young avocado trees tripled within a year. The height of avocado tree 2 increased from 3.60 m to 4.96 m and the total LA increased from 41.97 m^2 to 101.94 m^2 due to growth (Figure 7e), Table 4). The increasing canopy density may have caused some TLS occlusion. Therefore, the standard deviation of voxel level LAD increased from 2.84 m^2/m^3 to 3.14 m^2/m^3 (Figure 7d,d′, Table 4). The vertical leaf area of this avocado tree increased between 2.87 m^2 and 5.43 m^2, which was mainly detected within the height of 0.75 m to 4.5 m above ground (Figure 7e, Table 4). Additionally, LAD increased significantly at 2 m, 3 m and 4 m above ground height in the 13 months (Figure 8). Similarly, the height of avocado tree 1 increased from 3.66 m to 5.17 m and the total LA increased from 40.03 m^2 to 122.62 m^2 (Table 4). The standard deviation of voxel level LAD increased from 2.45 m^2/m^3 to 2.58 m^2/m^3 (Table 4). The vertical area of avocado tree 1 increased between 1.27 m^2 and 7.44 m^2 (Table 4), which was mainly detected within the height of 0.25 m to 4.75 m above ground. These two avocado trees were from the same research station, which were planted next to each other. They are the same variety, planted at the same density, and had the same management practices.

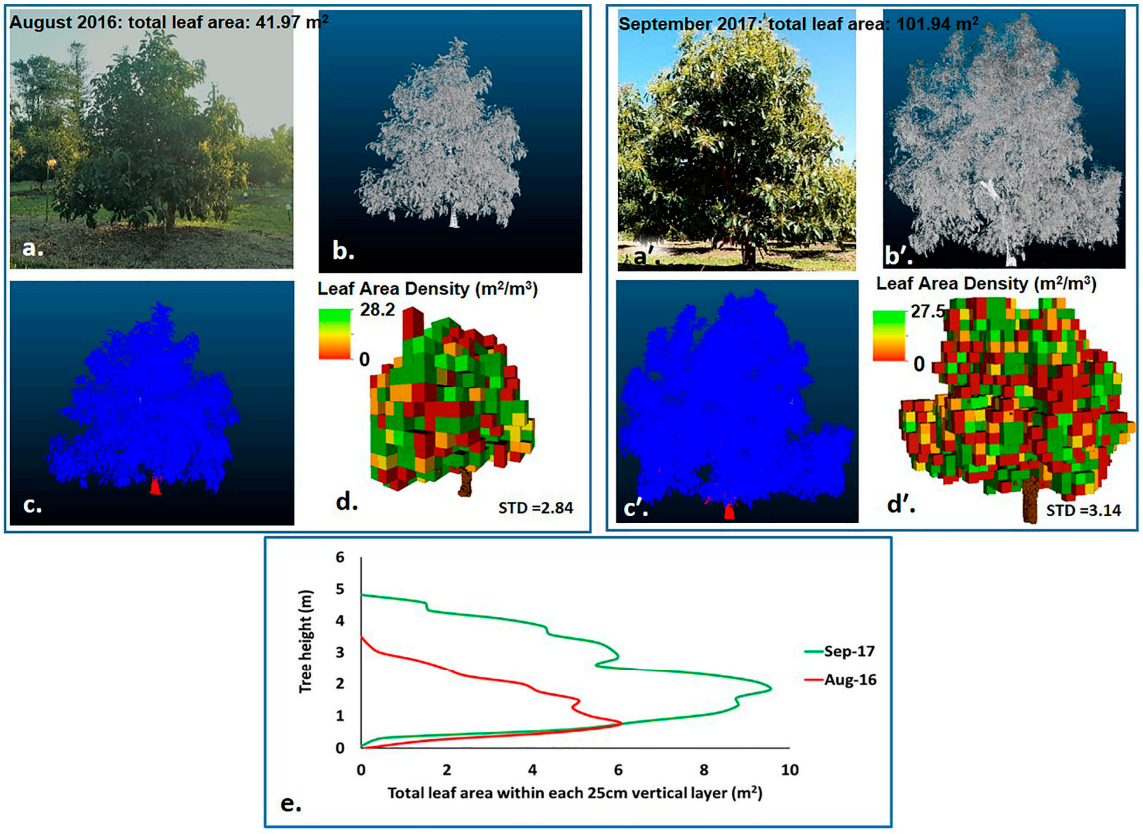

Figure 7. Pictures of an avocado tree, at two different points in time, approximately 13 months apart (**a**,**a′**), i.e., when the tree was two-year old and three-year old, its corresponding 3D intensity images (**b**,**b′**) and classified discrete point cloud (**c**,**c′**), leaf area density at a voxel level (25 cm in side length) (**d**,**d′**), and vertical leaf area profile within each 25 cm vertical layer (**e**).

Table 4. Structural properties and change of two small avocado trees when they were two and three years old.

Tree Number	Tree Height August 2016	Tree height September 2017	Leaf Area August 2016	Leaf Area September 2017	Standard Deviation of Voxel Level LAD in August 2016	Standard Deviation of Voxel Level LAD in September 2017	Leaf Area Increase Range of Each Vertical Layer
Avocado tree 1	3.66 m	5.17 m	40.03 m^2	122.62 m^2	2.45 m^2/m^3	2.58 m^2/m^3	1.27 m^2–7.44 m^2
Avocado tree 2	3.60 m	4.96 m	41.97 m^2	101.94 m^2	2.84 m^2/m^3	3.14 m^2/m^3	2.87 m^2–5.43 m^2

We used one young avocado tree as an example to investigate the influence of the voxel size on LA calculations at different growth stages, i.e., when the tree was two and three years old. LA was negatively related to the voxel size (Figure 9). The high correlation between LA and the voxel size provided potential to use a bigger voxel size to calculate the LA to save processing time. However, it also indicated that a significant error could occur if using an inappropriate voxel size. We considered the major contributors to the decreasing estimates of LA as a function of voxel size to be the non-random distribution of leaf material within big voxels and the lack of statistical consistency of small voxels. Big voxels may cause more vegetation clumping issues, which disobey the Beer-Lambert law hypothesis on the random and uniform distribution of leaf material within each voxel, which will cause calculation errors [43]. Small voxels may not capture a large enough number of sampling laser points, entering the voxel to provide a statistically consistent assessment for LA [43]. In spite of the influence of voxel size, the change of LA calculated at different voxel sizes was consistent (Figure 10). This indicated that if the focus is on relative LA changes, then the voxel size may not be a significant factor in our study. The LAD was also highly sensitive to voxel size. The mean LAD (computed on non-empty voxel) had a high negative correlation with voxel size (Figure 11).

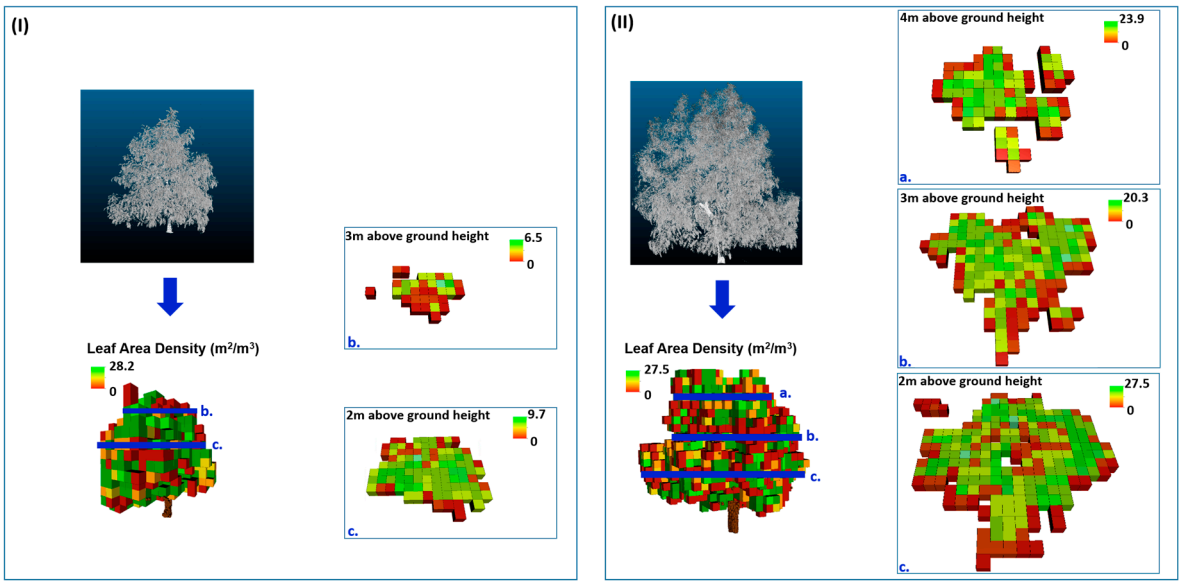

Figure 8. Intensity images of an avocado tree, at two different points in time, approximately 13 months apart (**I**,**II**), its corresponding leaf area density (LAD) of the entire tree crown, and LAD at 2 m, 3 m, and 4 m above ground height at the voxel level (25 cm in side length), when the tree was two-year old (**I**) and three-year old (**II**).

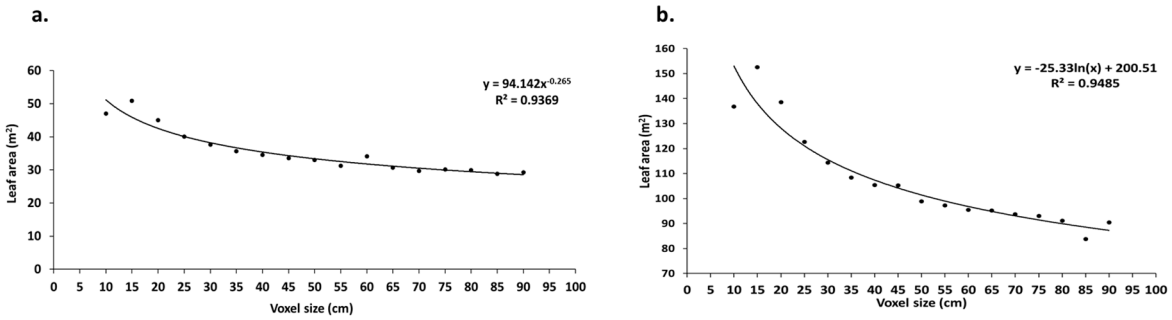

Figure 9. Leaf area of avocado tree when the tree was (**a**) two years old in August 2016 and (**b**) three years old in September 2017 for different voxel sizes.

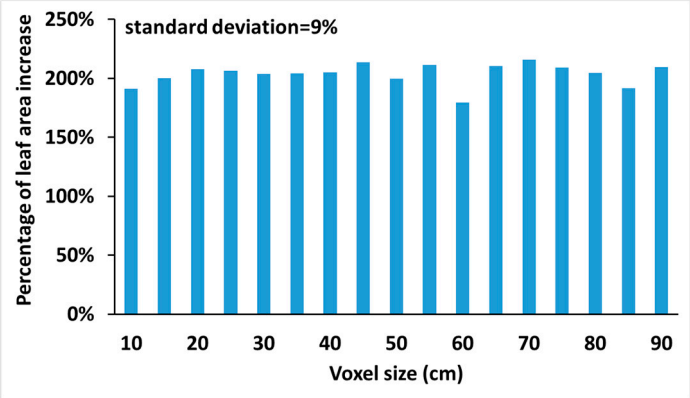

Figure 10. Percentage of leaf area increase of an avocado tree between August 2016 (two years old) and September 2017 (three years old) calculated at different voxel sizes.

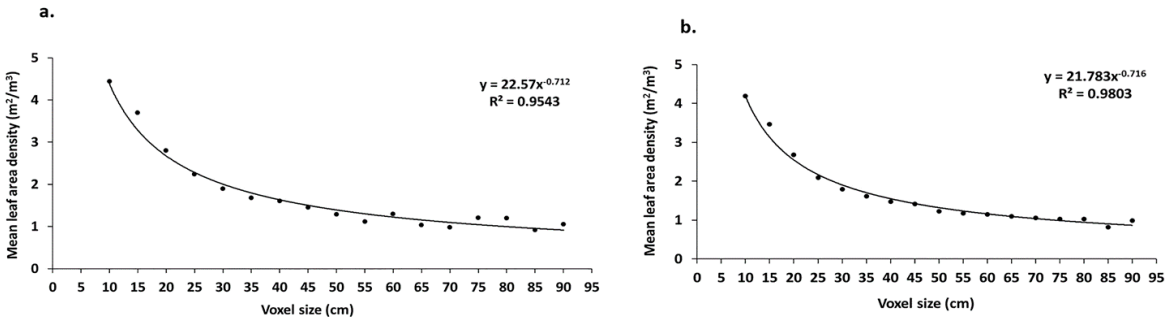

Figure 11. Mean leaf area density of an avocado tree when the tree was (**a**) two years old in August 2016 and (**b**) three years old in September 2017 for different voxel sizes.

5. Discussion

Mango, avocado and macadamia tree crops were selected for this study, as they provide three types of canopy structure complexities. Mango trees had the most simple canopy structure, while macadamia trees represented the most complicated canopy structure based on the number of leaves and branches within each tree crown (Figures 3–8). This study demonstrated that LA changes of mango, avocado, and macadamia tree crops could be determined from TLS data. Figures 3–8 illustrated that LA and LAD can be calculated at different heights. Having this ability to quantify these 3D differences in canopy structure complexity allows high spatial resolution TLS data to be used as a tool to assess horticultural tree crop changes due to phenology, management, weather and health conditions and to support the variable rate application of pesticides [20]. Furthermore, these tree crops also represented three levels of air and light interception requirements. For example, mango trees require the highest level of air circulation and light penetration due to the importance of fruit colour [44]. Mango growers open up the centre of the canopy through pruning to facilitate air circulation and light penetration and good airflow may also reduce disease outbreaks [44]. Hence, TLS derived structural measurements can also assist in achieving the optimal canopy openness for air circulation and light penetration.

LA and LAD are key factors for assessing growth and yield of mango, avocado and macadamia trees [45–47]. Therefore, LA and LAD calculations from TLS data (Table 2, Figures 3–8) may be useful to predict fruit yield and quality of macadamia, avocado, and mango trees. The ratio of leaves to fruit can significantly influence the flavour and quality of mangos [46,48]. Highly productive avocado varieties also require adequate LA for fruit development [45]. It is therefore essential to understand tree structural requirements for yield optimization.

AVG is a macadamia tree structure dysfunction that reduces nut production. It was originally found in Australia in the 1990s [19], and it has become a serious threat to macadamia orchards in Queensland and New South Wales in Australia. Although research on this has been done since 2002,

its causes are still unknown [19]. AVG directly modifies plant structure and can reduce yield by up to 30% [19,49]. Up to 100,000 macadamia trees were affected by AVG across Queensland and New South Wales in 2016, causing an annual loss of 10.5 million Australian dollars. Erect branches and poor flowering were found in macadamia trees affected with AVG [19], and these erected branches also made the macadamia trees more vulnerable to strong winds and storms. The LA and LAD results for the macadamia tree with AVG demonstrated that high spatial resolution TLS data has the potential to quantify storm damage and record where damage has occurred (Figure 5). For example, from September to December 2017, a significant increase in LA was expected due to flowering and spring flush. However, our study showed that LA of the macadamia tree with AVG decreased 10% while the healthy macadamia tree was able to withstand the storm and increase its LA by more than 50% during the same period (Table 2, Figure 5). The main loss of leaves for the macadamia tree with AVG was detected between 1.5 and 4.5 m above ground height, with substantial loss also noted at the top of tree crown (Figure 5e). This was attributed to the direct exposure of the apex to high wind speeds and hail damage during the storm.

Voxel level LAD calculation from high spatial resolution TLS data can potentially be used to test the effectiveness of pruning. The structure of horticultural tree crops can be adjusted via targeted limb removal or trellising that has been shown to improve their plant functions [50]. For example, young macadamia trees were trained to grow horizontally to become fruiting branches [51]. Modified tree pruning and branch training systems have been suggested for macadamia, avocado, and mango trees to achieve increased light interception and uniform light distribution [51–53]. We observed a decrease in the standard deviations of LAD for mango (Figure 3d,d′) and macadamia trees after pruning, which indicates that pruning may have reduced foliage clumping within the canopy.

TLS technology can automatically collect 3D crop structure data, which will contribute to further development of functional-structural plant modelling (FSPM) and it can be used for validation purposes of traditional methods. Many studies have been conducted to understand crop growth, the effect of environmental conditions, as well as how genetic variations influence the resilience of tree crops [50]. The ability of practical and accurate tools to calculate precise geometric characteristics of tree crops will help develop better crop training systems and to understand the genetic variations between tree crops. FSPM was developed in the 1990s to illustrate changes of plant structure in 3D [50] and has been applied to tree crops such as macadamias [54]. The traditional way to acquire 3D structural information was to manually measure branch and leaf structure, which is regarded as tedious and error-prone [49,54]. TLS technology can automate 3D crop structure data collection, providing detailed and accurate data with high spatial and temporal resolutions [55,56]. Furthermore, measurements can be done in either an indoor or outdoor environment. Our study has indicated that TLS can successfully identify different plant parts (e.g., leaves and branches) and show LA changes (Figure 3c,c′, Figure 5c,c′, Figure 7c,c′).

One limitation of using high spatial resolution TLS is the labour, cost of equipment, level of technological and analytical knowledge, and time required to set up and operate the scanner and its ground control. Hence, this study was restricted to six trees. However, the emerging application of unmanned aerial vehicle (UAV) LiDAR may also improve data acquisition efficacies in the near future. The RIEGL RiCOPTER can produce comparable canopy height models and DBH results [57] to the RIEGL VZ-400, which was used for this study. Thus, UAV based LiDAR data has the potential to be used for scaling up the accurate geometrical canopy structure measurements from TLS, which would provide information for precision nutrition, irrigation, and fertilisation applications [16]. Another limitation of this research is that we did not validate the LAD or LA results against reference data. LA reference data can be collected by both direct and indirect methods. Indirect LA measurement method (e.g., using the LAI 2200 canopy analyser and hemispherical image cameras) integrates both leaves and branches to infer LA measurement, which becomes an estimation of plant area instead [43]. In addition, another limitation of the LAI 2200 canopy analyser is that it is based on gap probabilities at different zenith angles to estimate an LAI within the covered area, which is only for continuous

forests measurements. Therefore, the indirect LA method cannot be used to validate the LA results from this research. Although allometric relationships have been widely applied in forest area [58], the allometric relationship can be rigid for horticultural tree crops due to genetic variation, environmental manipulation and pruning management [59]. How these factors influence the overall allometry of a horticultural tree is unkown [59]. Brym et al. [59] explored a process-based method for two species of apple trees, but allometric relationships were only applicable for branch mass and diameter. The direct destructive method, measuring individual leaves, would be the only way to validate the LA calculation in this study [60]. Consecutive manual pruning of canopies at voxel level to investigate measured LA changes is suggested as a direction for future work. However, this method is impractical in a commercial orchard environment, and for our study this option was not available. It seems that the change of LA at different growth stages calculated at different voxel sizes was consistent in our study (Figure 11). Therefore, the change analysis and discussion were based on the LAD and LA results calculated from the 25 cm side length of voxels as examples. However, the analysis of the voxel size effects on LA changes in this study was only based on a single avocado tree. Therefore, future work should undertake further experiments on additional tree crops to determine if our observed results are consistent. Although there are a variety of factors that influence the optimal sampling voxel size, such as leaf size, branch architecture, and occlusion effect [61], there is no clear standard to identify the optimal voxel size. Our results relied on the accuracies reported in previous studies, e.g., [6,22]. Furthermore, factors including canopy density, leaf sizes and angles need to be taken into consideration separately to calculate LA and LAD for each of the tree crops in future studies.

6. Conclusions

This study assessed the ability of TLS to calculate LA and LAD of mango, avocado, and macadamia tree crops. The LA changes calculated from TLS data were consistent with the expected LA changes caused by canopy management, growth and a severe storm. Voxel level LAD calculations not only allowed us to measure leaf distribution, but also quantify LA at a specific height of the canopy. Therefore, TLS may be a useful tool to quantify horticultural tree LA changes over time, which can be used to understand tree growth and productivity, targetted limb removal to maximise light interception, irrigation, and fertilisation applications. Further research should be directed to upscale these measurements to the orchard level. The evaluation of TLS technologies over the three types of canopy structure complexities with differing air and sunlight penetration requirements demonstrates the applicability of this technology to other tree crop species.

Author Contributions: D.W., S.P., K.J., and A.R. jointly conceived and designed this study; D.W. lead the field data collection with the contribution of K.J., S.P., C.S., and A.R.; D.W. processed and analysed the data and led the writing of the paper with all authors making contributions.

Funding: This research was funded by Department of Agriculture and Water Resources, Australian Government as part of its Rural R&D for Profit Program's subproject "Multi-Scale Monitoring Tools for Managing Australia Tree Crops—Industry Meets Innovation".

Acknowledgments: The authors acknowledge the Australian Federal Government 'Rural R and D for Profit' scheme and Horticulture Innovation Australia for funding this Research. The authors appreciate the support provided for this research by Simpson Farms Pty. Ltd. (Childers, QLD 4660, Australia), in particular, Chad Simpson, Bundaberg Research Facility, the Queensland Government's Department of Agriculture and Fisheries, in particular, John Wilkie and Helen Hofman. We thank Martin Béland for sharing the Matlab code to calculate the leaf area density, Peter Scarth for Matlab assistance and Nicholas Goodwin for assisting data registration. We also thank Aaron Aeberli and Yu-Hsuan Tu for their assistance with fieldwork and Eva Kovacs for editing the manuscript.

Conflicts of Interest: The authors declare no conflict of interest.

References

1. Lovell, J.L.; Jupp, D.L.B.; Newnham, G.J.; Culvenor, D.S. Measuring tree stem diameters using intensity profiles from ground-based scanning lidar from a fixed viewpoint. *ISPRS J. Photogramm. Remote Sens.* **2011**, *66*, 46–55. [CrossRef]
2. Calders, K.; Schenkels, T.; Bartholomeus, H.; Armston, J.; Verbesselt, J.; Herold, M. Monitoring spring phenology with high temporal resolution terrestrial lidar measurements. *Agric. For. Meteorol.* **2015**, *203*, 158–168. [CrossRef]
3. Newnham, G.J.; Armston, J.D.; Calders, K.; Disney, M.I.; Lovell, J.L.; Schaaf, C.B.; Strahler, A.H.; Danson, F.M. Terrestrial laser scanning for plot-scale forest measurement. *Curr. For. Rep.* **2015**, *1*, 239–251. [CrossRef]
4. Danson, F.M.; Gaulton, R.; Armitage, R.P.; Disney, M.; Gunawan, O.; Lewis, P.; Pearson, G.; Ramirez, A.F. Developing a dual-wavelength full-waveform terrestrial laser scanner to characterize forest canopy structure. *Agric. For. Meteorol.* **2014**, *198–199*, 7–14. [CrossRef]
5. Wang, W.; Zhao, W.; Huang, L.; Vimarlund, V.; Wang, Z. Applications of terrestrial laser scanning for tunnels: A review. *J. Traffic Transp. Eng.* **2014**, *1*, 325–337. [CrossRef]
6. Béland, M.; Widlowski, J.-L.; Fournier, R.A. A model for deriving voxel-level tree leaf area density estimates from ground-based lidar. *Environ. Model. Softw.* **2014**, *51*, 184–189. [CrossRef]
7. Li, S.; Dai, L.; Wang, H.; Wang, Y.; He, Z.; Lin, S. Estimating leaf area density of individual trees using the point cloud segmentation of terrestrial lidar data and a voxel-based model. *Remote Sens.* **2017**, *9*, 1202. [CrossRef]
8. Srinivasan, S.; Popescu, S.; Eriksson, M.; Sheridan, R.; Ku, N.-W. Terrestrial laser scanning as an effective tool to retrieve tree level height, crown width, and stem diameter. *Remote Sens.* **2015**, *7*, 1877. [CrossRef]
9. Jupp, D.L.B.; Culvenor, D.S.; Lovell, J.L.; Newnham, G.J.; Strahler, A.H.; Woodcock, C.E. Estimating forest LAI profiles and structural parameters using a ground-based laser called 'Echidna'. *Tree Physiol.* **2009**, *29*, 171–181. [CrossRef] [PubMed]
10. Calders, K.; Armston, J.; Newnham, G.; Herold, M.; Goodwin, N. Implications of sensor configuration and topography on vertical plant profiles derived from terrestrial lidar. *Agric. For. Meteorol.* **2014**, *194*, 104–117. [CrossRef]
11. Kaasalainen, S.; Krooks, A.; Liski, J.; Raumonen, P.; Kaartinen, H.; Kaasalainen, M.; Puttonen, E.; Anttila, K.; Mäkipää, R. Change detection of tree biomass with terrestrial laser scanning and quantitative structure modelling. *Remote Sens.* **2014**, *6*, 3906–3922. [CrossRef]
12. Calders, K.; Newnham, G.; Burt, A.; Murphy, S.; Raumonen, P.; Herold, M.; Culvenor, D.; Avitabile, V.; Disney, M.; Armston, J. Nondestructive estimates of above-ground biomass using terrestrial laser scanning. *Methods Ecol. Evol.* **2015**, *6*, 198–208. [CrossRef]
13. Raumonen, P.; Kaasalainen, M.; Åkerblom, M.; Kaasalainen, S.; Kaartinen, H.; Vastaranta, M.; Holopainen, M.; Disney, M.; Lewis, P. Fast automatic precision tree models from terrestrial laser scanner data. *Remote Sens.* **2013**, *5*, 491–520. [CrossRef]
14. Hancock, S.; Anderson, K.; Disney, M.; Gaston, K.J. Measurement of fine-spatial-resolution 3d vegetation structure with airborne waveform lidar: Calibration and validation with voxelised terrestrial lidar. *Remote Sens. Environ.* **2017**, *188*, 37–50. [CrossRef]
15. Greaves, H.E.; Vierling, L.A.; Eitel, J.U.H.; Boelman, N.T.; Magney, T.S.; Prager, C.M.; Griffin, K.L. Applying terrestrial lidar for evaluation and calibration of airborne lidar-derived shrub biomass estimates in arctic tundra. *Remote Sens. Lett.* **2017**, *8*, 175–184. [CrossRef]
16. Rosell, J.; Sanz, R. A review of methods and applications of the geometric characterization of tree crops in agricultural activities. *Comput. Electron. Agric.* **2012**, *81*, 124–141. [CrossRef]
17. Lee, K.-H.; Ehsani, R. A laser scanner based measurement system for quantification of citrus tree geometric characteristics. *Appl. Eng. Agric.* **2009**, *25*, 777–788. [CrossRef]
18. Sinoquet, H.; Stephan, J.; Sonohat, G.; Lauri, P.É.; Monney, P. Simple equations to estimate light interception by isolated trees from canopy structure features: Assessment with three-dimensional digitized apple trees. *New Phytol.* **2007**, *175*, 94–106. [CrossRef] [PubMed]
19. O'Farrell, P.; Le Lagadec, D.; Searle, C. 'Abnormal vertical growth': A disorder threatening the viability of the australian macadamia industry. *Acta Hortic.* **2016**, *1109*, 143–150. [CrossRef]

20. Palacin, J.; Pallejà, T.; Tresanchez, M.; Sanz, R.; Llorens Calveras, J.; Ribes-Dasi, M.; Masip, J.; Arnó, J.; Escolà, A.; Ramon Rosell, J. Real-time tree-foliage surface estimation using a ground laser scanner. *IEEE Trans. Instrum. Meas.* **2007**, *56*, 1377–1383. [CrossRef]
21. Gucci, R.; Cantini, C. *Pruning and Training Systems for Modern Olive Growing*; CSIRO Publishing: Collingwood, Australia, 2000.
22. Béland, M.; Widlowski, J.-L.; Fournier, R.A.; Côté, J.-F.; Verstraete, M.M. Estimating leaf area distribution in savanna trees from terrestrial lidar measurements. *Agric. For. Meteorol.* **2011**, *151*, 1252–1266. [CrossRef]
23. Jagbrant, G.; Underwood, J.P.; Nieto, J.; Sukkarieh, S. Lidar based tree and platform localisation in almond orchards. In *Field and Service Robotics*; Springer: New York, NY, USA, 2015; pp. 469–483.
24. Underwood, J.P.; Hung, C.; Whelan, B.; Sukkarieh, S. Mapping almond orchard canopy volume, flowers, fruit and yield using lidar and vision sensors. *Comput. Electron. Agric.* **2016**, *130*, 83–96. [CrossRef]
25. Arnó, J.; Escolà, A.; Masip, J.; Rosell-Polo, J.R. Influence of the scanned side of the row in terrestrial laser sensor applications in vineyards: Practical consequences. *Precis. Agric.* **2015**, *16*, 119–128. [CrossRef]
26. Del-Moral-Martínez, I.; Rosell-Polo, J.R.; Company, J.; Sanz, R.; Escolà, A.; Masip, J.; Martínez-Casasnovas, J.A.; Arnó, J. Mapping vineyard leaf area using mobile terrestrial laser scanners: Should rows be scanned on-the-go or discontinuously sampled? *Sensors* **2016**, *16*, 119. [CrossRef] [PubMed]
27. Hosoi, F.; Omasa, K. Factors contributing to accuracy in the estimation of the woody canopy leaf area density profile using 3d portable lidar imaging. *J. Exp. Bot.* **2007**, *58*, 3463–3473. [CrossRef] [PubMed]
28. Brodu, N.; Lague, D. 3d terrestrial lidar data classification of complex natural scenes using a multi-scale dimensionality criterion: Applications in geomorphology. *ISPRS J. Photogramm. Remote Sens.* **2012**, *68*, 121–134. [CrossRef]
29. Siegfried, W.; Viret, O.; Huber, B.; Wohlhauser, R. Dosage of plant protection products adapted to leaf area index in viticulture. *Crop Prot.* **2007**, *26*, 73–82. [CrossRef]
30. Furness, G.O.; Magarey, P.A.; Miller, P.M.; Drew, H.J. Fruit tree and vine sprayer calibration based on canopy size and length of row: Unit canopy row method. *Crop Prot.* **1998**, *17*, 639–644. [CrossRef]
31. Llop, J.; Gil, E.; Llorens, J.; Miranda-Fuentes, A.; Gallart, M. Testing the suitability of a terrestrial 2d lidar scanner for canopy characterization of greenhouse tomato crops. *Sensors* **2016**, *16*, 1435. [CrossRef] [PubMed]
32. Gil, E.; Arnó, J.; Llorens, J.; Sanz, R.; Llop, J.; Rosell-Polo, J.R.; Gallart, M.; Escolà, A. Advanced technologies for the improvement of spray application techniques in spanish viticulture: An overview. *Sensors* **2014**, *14*, 691–708. [CrossRef] [PubMed]
33. Gladstone, E.A.; Dokoozlian, N.K. Influence of leaf area density and trellis/training system on the light microclimate within grapevine canopies. *VITIS-GEILWEILERHOF-* **2003**, *42*, 123–131.
34. Bundaberg Fruit & Vegetable Growers. Bundaberg Fruit & Vegetable Growers. Available online: https://www.bfvg.com.au/ (accessed on 15 October 2018).
35. Australia Mango Industry Association Ltd., Horticulture Australia. Australian Mango Industry Strategic Investment Plan 2014/15–2018/19; 30 May 2014. Available online: https://static1.squarespace.com/static/53b0ef57e4b04ed3debabc4f/t/540cdb46e4b068678cd375f9/1410128710084/Strategic+Investment+Plan+2014+15+to+2018+19+-+Mango.pdf (accessed on 10 June 2018).
36. Queensland Government. Mangoes. Available online: https://www.daf.qld.gov.au/plants/fruit-and-vegetables/fruit-and-nuts/mangoes (accessed on 19 August 2018).
37. Horticulture Innovation Australia. Find Information, Publications, Industry Contacts and More on the Avocado Industry. Available online: http://horticulture.com.au/grower-focus/avocado/ (accessed on 11 July 2016).
38. Avocados Australia. Australian Avos in Your Burger and on Your Pizza—21/09/2010. Available online: http://industry.avocado.org.au/NewsItem.aspx?NewsId=51 (accessed on 11 July 2016).
39. Australia Macadamia Society. Australia Macadamia Society Factsheet, Bundaberg, QLD. Available online: https://app-ausmacademia-au-syd.s3.ap-southeast-2.amazonaws.com/abouttiles/IhiLOa09ER4XkGPp4JiYWevNzHYV9Ft1dmsoRGKN.pdf (accessed on 6 November 2018).
40. Ma, L.; Zheng, G.; Eitel, J.U.H.; Magney, T.S.; Moskal, L.M. Determining woody-to-total area ratio using terrestrial laser scanning (TLS). *Agric. For. Meteorol.* **2016**, *228–229*, 217–228. [CrossRef]
41. Robson, A.; Rahman, M.; Muir, J. Using worldview satellite imagery to map yield in avocado (*Persea americana*): A case study in Bundaberg, Australia. *Remote Sens.* **2017**, *9*, 1223. [CrossRef]
42. Bureau of Meteorology. Bundaberg, Queensland, November 2017 Daily Weather Observations. Available online: http://www.bom.gov.au/climate/dwo/201711/html/IDCJDW4021.201711.shtml (accessed on 18 June 2018).

43. Grau, E.; Durrieu, S.; Fournier, R.; Gastellu-Etchegorry, J.-P.; Yin, T. Estimation of 3d vegetation density with terrestrial laser scanning data using voxels. A sensitivity analysis of influencing parameters. *Remote Sens. Environ.* **2017**, *191*, 373–388. [CrossRef]
44. Poffley, M.; Owens, G. Mango Pruning in the Top End Resources. 2006; p. 4. Available online: https://dpir.nt.gov.au/__data/assets/pdf_file/0018/232920/598.pdf (accessed on 1 May 2018).
45. Schaffer, B.; Schaffer, B.; Whiley, A.W.; Wolstenholme, B.N. *The Avocado Botany, Production and Uses*, 2nd ed.; Schaffer, B.A., Wolstenholme, B.N., Whiley, A.W., Eds.; CABI: Wallingford, UK, 2013.
46. Ghoreishi, M.; Hossini, Y.; Maftoon, M. Simple models for predicting leaf area of mango (*Mangifera indica* L.). *J. Biol. Earth Sci.* **2012**, *2*, 9.
47. McFadyen, L.M.; Morris, S.G.; Oldham, M.A.; Huett, D.O.; Meyers, N.M.; Wood, J.; McConchie, C.A. The relationship between orchard crowding, light interception, and productivity in macadamia. *Aust. J. Agric. Res.* **2004**, *55*, 1029–1038. [CrossRef]
48. Simmons, S.L.; Hofman, P.J.; Whiley, A.W.; Hetherington, S.E. Effects of leaf: Fruit ratios on fruit growth, mineral concentration and quality of mango (*Mangifera indica* L. Cv. Kensington pride). *J. Hortic. Sci. Biotechnol.* **1998**, *73*, 367–374. [CrossRef]
49. Gibbs, J.A.; Pound, M.; French, A.P.; Wells, D.M.; Murchie, E.; Pridmore, T. Approaches to three-dimensional reconstruction of plant shoot topology and geometry. *Funct. Plant Biol.* **2016**, *44*, 62–75. [CrossRef]
50. Vos, J.; Evers, J.B.; Buck-Sorlin, G.H.; Andrieu, B.; Chelle, M.; de Visser, P.H.B. Functional–structural plant modelling: A new versatile tool in crop science. *J. Exp. Bot.* **2010**, *61*, 2101–2115. [CrossRef] [PubMed]
51. Huett, D. Macadamia physiology review: A canopy light response study and literature review. *Crop Pasture Sci.* **2004**, *55*, 609–624. [CrossRef]
52. Stassen, P.; Davie, S.; Snijder, B. Training young hass avocado trees into a central leader for accommodation in higher density orchards. In Proceedings of the World Avocado Congress III, Tel Aviv, Israel, 22–27 October 1995; p. 254.
53. Campbell, R.J.; Wasielewski, J. *Mango Tree Training Techniques for the Hot Tropics*; International Society for Horticultural Science (ISHS): Leuven, Belgium, 2000; pp. 641–652.
54. White, N.; Hanan, J. Use of Functional-Structural Plant Modelling in Horticulture. 2012. Available online: https://www.researchgate.net/publication/230877125_Use_of_Functional-Structural_Plant_Modelling_in_Horticulture (accessed on 10 June 2018).
55. Eitel, J.U.H.; Höfle, B.; Vierling, L.A.; Abellán, A.; Asner, G.P.; Deems, J.S.; Glennie, C.L.; Joerg, P.C.; LeWinter, A.L.; Magney, T.S.; et al. Beyond 3-d: The new spectrum of lidar applications for earth and ecological sciences. *Remote Sens. Environ.* **2016**, *186*, 372–392. [CrossRef]
56. Hackenberg, J.; Spiecker, H.; Calders, K.; Disney, M.; Raumonen, P. Simpletree—An efficient open source tool to build tree models from tls clouds. *Forests* **2015**, *6*, 4245–4294. [CrossRef]
57. Brede, B.; Lau, A.; Bartholomeus, H.; Kooistra, L. Comparing RIEGL RiCOPTER UAV LiDAR derived canopy height and DBH with terrestrial LiDAR. *Sensors* **2017**, *17*, 2371. [CrossRef] [PubMed]
58. Forrester, D.I.; Tachauer, I.H.H.; Annighoefer, P.; Barbeito, I.; Pretzsch, H.; Ruiz-Peinado, R.; Stark, H.; Vacchiano, G.; Zlatanov, T.; Chakraborty, T.; et al. Generalized biomass and leaf area allometric equations for european tree species incorporating stand structure, tree age and climate. *For. Ecol. Manag.* **2017**, *396*, 160–175. [CrossRef]
59. Brym, Z.T.; Ernest, S.K.M. Process-based allometry describes the influence of management on orchard tree aboveground architecture. *PeerJ* **2018**, *6*, e4949. [CrossRef] [PubMed]
60. Woodgate, W.; Armston, J.D.; Disney, M.; Jones, S.D.; Suarez, L.; Hill, M.J.; Wilkes, P.; Soto-Berelov, M. Quantifying the impact of woody material on leaf area index estimation from hemispherical photography using 3d canopy simulations. *Agric. For. Meteorol.* **2016**, *226–227*, 1–12. [CrossRef]
61. Béland, M.; Baldocchi, D.D.; Widlowski, J.-L.; Fournier, R.A.; Verstraete, M.M. On seeing the wood from the leaves and the role of voxel size in determining leaf area distribution of forests with terrestrial lidar. *Agric. For. Meteorol.* **2014**, *184*, 82–97. [CrossRef]